


Combined Ultrasound Treatment with Transferrin-Coupled Nanoparticles Improves Active Targeting of 4T1 Mammary Carcinoma Cells

Technology in Cancer Research & Treatment
 Volume 20: 1-10
 © The Author(s) 2021
 Article reuse guidelines:
sagepub.com/journals-permissions
 DOI: 10.1177/15330338211062325
journals.sagepub.com/home/tct


Xiangzi Jin*, Jie Yu*, Meijiao Yin, Amit Sinha, and Guangming Jin 

Abstract

Objective: Conventional chemotherapy remains the mainstay treatment for many breast cancer patients, but its effectiveness is limited by toxic side effects. Incorporating drugs such as docetaxel into nanoparticle medicines can reduce toxicity but further improvements are required. To facilitate more active tumor targeting, we prepared transferrin-docetaxel-loaded pegylated-albumin nanoparticles (Tf-PEG-DANPS). **Methods:** The growth inhibitory effects and the ability of unmodified DANPS or PEG-DANPS to induce apoptosis in 4T1 mouse mammary cancers were compared to Tf-PEG-DANPS treatment using 3-(4,5-dimethylthiazol-2-yl)-2,5-diphenyltetrazolium bromide (MTT) and flow cytometry. These experiments were extended in vivo to the intravenous treatment of 4T1 tumors where PEG-DANPS was compared to Tf-PEG-DANPS alone or Tf-PEG-DANPS combined with ultrasound (US + Tf-PEG-DANPS). Histological assessments using hematoxylin and eosin (HE) sections were performed to examine antitumor activity, metastasis to lung and liver, and body weight measurements taken as an indicator of toxicity. **Results:** MTT experiments show that, in the normal and low concentration interval, the inhibition ability of the Tf-PEG-DANPS is higher than that of other drug-giving groups, and the flow cytometry show that the proportion of induced apoptosis in each given group is 2.88%, 42.95%, 48.23%, and 57.89%, indicating that the Tf-PEG-DANPS group has more significant ability to induce apoptosis than other drug-giving groups. From the pathological HE staining and semiquantitative analysis, US+Tf-PEG-DANPS can effectively inhibit the growth of breast cancer transplanted tumors and suppress metastases, it also has smaller toxic side effects on mice. **Conclusion:** The antitumor effect of US+Tf-PEG-DANPS represents an effective combination that exhibits increased antitumor activity and metastasis reduction with an improved side-effect profile.

Keywords

breast cancer, docetaxel-albumin nanoparticles, polyethylene glycol, transferrin, ultrasound

Abbreviations

HE, hematoxylin and eosin; MTT, measured using the 3-(4,5-dimethylthiazol-2-yl)-2,5-diphenyltetrazolium bromide; PEG-DANPS, pegylated-albumin nanoparticles; PI, propidium iodide; RES, reticuloendothelial system; TEM, transmission electron microscopy; Tf, transferrin; Tf-PBS, Tf-phosphate-buffered saline; Tf-PEG-DANPS, transferrin-docetaxel-loaded pegylated-albumin nanoparticles; US, ultrasound

Received: July 22, 2021; Revised: October 13, 2021; Accepted: November 4, 2021.

Introduction

Breast cancer is a serious threat to women's health, it is the most common cancer among women in China and the sixth leading cause of cancer-related deaths.¹ Worldwide, the incidence rate for breast cancer in 2018 accounted for 11.6% of all cancers, making it the second most common cancer in the world population.² Among these cases, nearly two-thirds present with advanced-stage disease and 82.1% of patients are symptomatic

at diagnosis.³ Surgery and chemotherapy are still the primary

Yanbian University Hospital, Yanji 133000, China

*Contributed equally.

Corresponding Author:

Guangming Jin, Yanbian University Hospital, Yanji 133000, China.
 Email: jgm920@sina.com



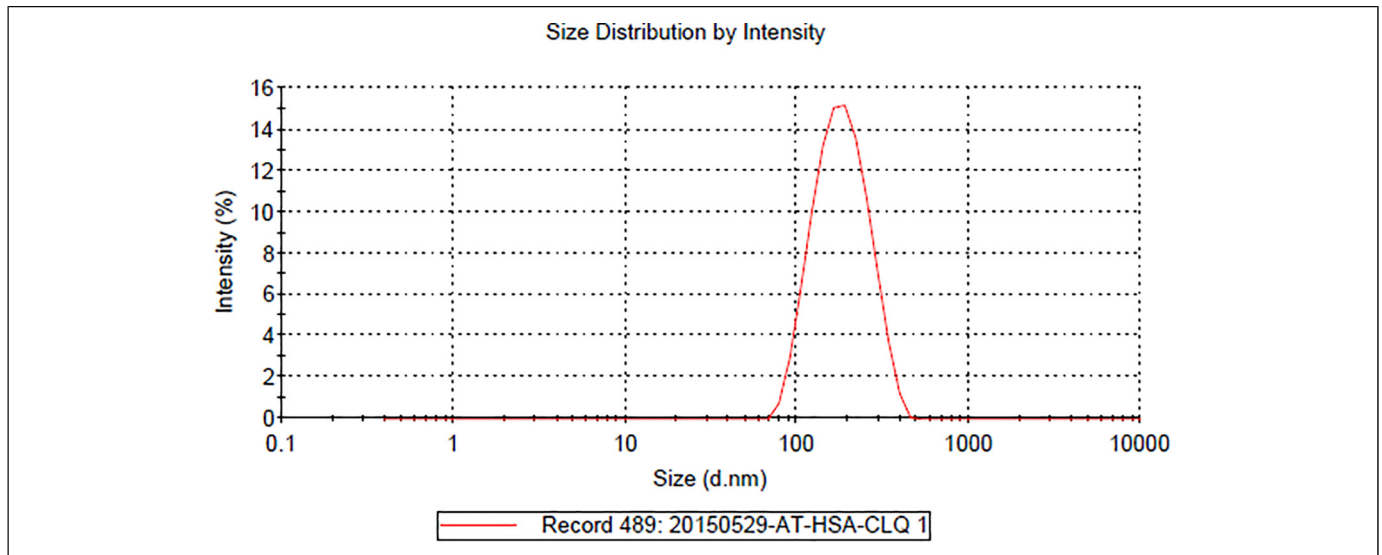


Figure 1. Particle size of transferrin-docetaxel-loaded pegylated-albumin nanoparticles (Tf-PEG-DANPS; 164.3 ± 3.58 nm).

treatments, however, 12.1% of patients receive <4 cycles of chemotherapy due to their toxic effects, a situation which is well below international minimum standards.^{4,5} Toward this, previous research using docetaxel-loaded pegylated-albumin nanoparticles (PEG-DANPS) showed that this formulation avoided sequestration by the reticuloendothelial system (RES) during the therapy of nonsmall-cell lung cancer. This improved targeting of cancer cells,^{6,7} but the docetaxel was still distributed in normal tissues.

According to relevant research, the transferrin receptor (TfR) is overexpressed in breast cancer.⁸ Therefore, some scholars have

proposed a concept to connect the drug with the specific receptor of TfR—transferrin (Tf). They think that will allow the drug to bind specifically to the tumor and ultimately target the tumor cells. Şenay had treated the tumor by ultrasound (US) in combination with anticancer drugs, revealing that the impact of cavitation of US can push the drug directly into the cancer cells, thus greatly enhancing drug absorption.⁹ These studies provide us with ideas for further research. On the basis of previous studies, the Tf-pegylated docetaxel-albumin nanoparticles (Tf-PEG-DANPS) will be prepared first, and then the US will be used for adjuvant therapy of a breast cancer mouse model, hoping to achieve the dual goals of improving drug targeting and increasing drug absorption.

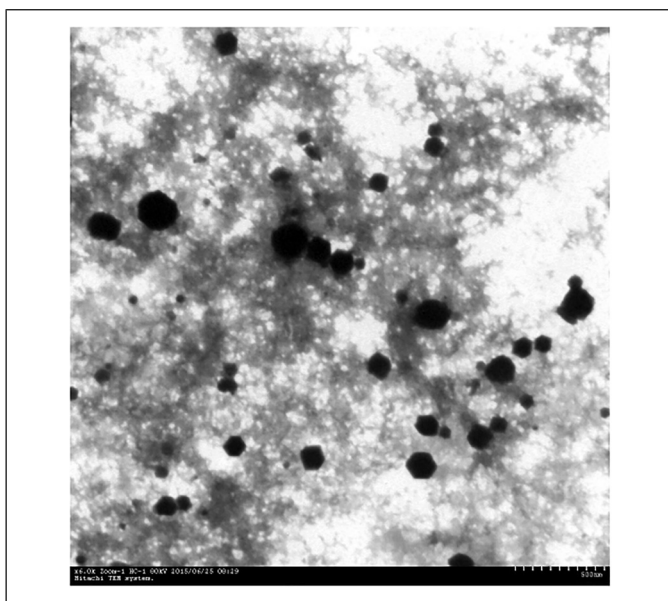


Figure 2. TEM scanning of blank Tf-PEG-DANPS ($\times 300,000$). Abbreviations: TEM, transmission electron microscopy; Tf-PEG-DANPS, transferrin-docetaxel-loaded pegylated-albumin nanoparticles.

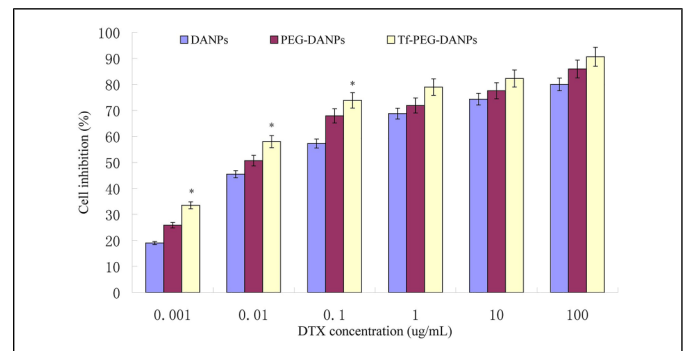


Figure 3. Growth inhibitory effects of DANPS, PEG-DANPS, and Tf-PEG-DANPS treatments on 4T1 cells. Cell proliferation was measured after 48 h after treatment with the indicated doses (0.001-0.1 $\mu\text{g/mL}$) and expressed relative to the untreated control (5% glucose).

Abbreviations: DANPS: docetaxel-albumin nanoparticles; PEG-DANPS: docetaxel-loaded pegylated-albumin nanoparticles; Tf-PEG-DANPS: transferrin-PEG-DANPS.

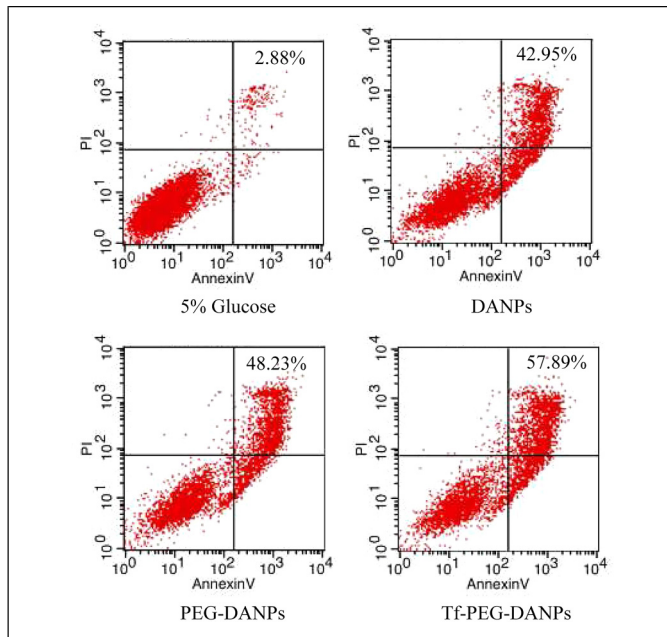


Figure 4. Induction of apoptosis in 4T1 cells after treatment with DANPs, PEG-DANPs, or Tf-PEG-DANPs. Cells were treated with 10 10 $\mu\text{g}/\text{mL}$ of each agent or a control (5% glucose) for 48 h and apoptosis was measured using flow cytometry.

Abbreviations: DANPs: docetaxel-albumin nanoparticles; PEG-DANPs: docetaxel-loaded pegylated-albumin nanoparticles; Tf-PEG-DANPs: transferrin-PEG-DANPs.

Materials and Methods

Cell Line and Animals

The 4T1 murine mammary cancer cell line was provided by the Department of Pathology, Institute of Medicinal Biotechnology in Peking Union Medical College. Balb/c female mice were purchased from Beijing Vital River Laboratories (4-7 weeks old, 18-20 g, SPF Clean Rating, production license SCXK 2016-0006, use license SYXK 2014-0023). All mice were housed under pathogen-free laboratory conditions (12 h light/12 h dark schedule, temperature 18-22 °C, humidity 50%-60%) and fed autoclaved Harlan Teklad Sterilizable rodent diet (Beijing Huafukang Biotechnology Co. Ltd, license number: SCXK 2014-0015) and pure water. Mice were monitored

Table 1. Apoptosis index of A549 cells by in situ terminal labeling ($\bar{x} \pm s$).

Group	Vision	AI%
Control group	15	3.22 \pm 5.23
DANPs group	15	33.22 \pm 6.01
PEG-DANPs group	15	55.61 \pm 4.88
US + PEG-DANPs group	15	70.35 \pm 5.76*

Abbreviations: DANPs, docetaxel-albumin nanoparticles; PEG-DANPs, docetaxel-loaded pegylated-albumin nanoparticles; US-PEG-DANPs, PEG-DANPs combined with ultrasound.

Note. Compared with other groups, * $P < .05$.

daily, including abnormal postural gait, mental state, appetite, weight change, urine and feces character, and tumor size. The reporting of this study conforms to ARRIVE 2.0 guidelines. (5967836).¹⁰ All animal procedures were approved by the institutional ethics committee (Regulations on Administration and Protection of experimental animals), Yanbian University Hospital under the approval number IACUC-202002022-05. All experiments abided by the Ethical 3R principle. We commit that we had made our best efforts to minimize the number of animals utilized and to decrease their suffering.¹¹

Reagents and Instruments

DANPs, PEG-DANPs, fetal bovine serum, trypsin, and Dulbecco minimum essential medium were purchased from Longrun Technology Co. Ltd and phosphate-buffered saline was purchased from Thermo Scientific. All organic solvents used were of analytical purity grade. The following instruments were used as indicated in the study: NANO DEBEE45 1 milk homogenizer (NANO), DZF-200 vacuum drier (Pudong Rongfeng Scientific Instrument Co. Ltd), IKA MS3 vortex (Malvern), Agilent Tech 1200 high-performance liquid chromatography (Agilent), V-999H Rotary evaporator (Buchi), Spectra Max190 Enzyme Marker (Tecan), HERA Cell 150 cell incubator (HERA), Thermo micro max high-speed centrifuge (Hitachi), and low-intensity nonfocusing ultrasonic instrument (Siemens).

Preparation of Tf-PEG-DANPs

Tf-PEG-DANPs was prepared by electrostatic attraction and lipophilic reaction. Briefly, lyophilized PEG-DANPs preparations were subjected to sequential addition of 5% glucose solution according to the ratio of 3:1 for stirring and 1 mL of Tf-phosphate-buffered saline (PBS) solution, added slowly and stirred thoroughly at 400 r/min before centrifugation for 10 min ($r = 8$ cm). Preparations were separated by gel filtration chromatography using a Sephadex G-50 column and filtered through a 0.45 μm membrane. Tf-PEG-DANPs was then freeze-dried and reconstituted in a 5% glucose solution prior to experimental use.

Cell Proliferation Assays

The effect of the nanoparticle preparations on cell proliferation was measured using the 3-(4,5-dimethylthiazol-2-yl)-2,5-diphenyltetrazolium bromide (MTT) method. Briefly, 4T1 cells (8×10^4 cells/well) were seeded into 96-well plates. After 24 h, cells were treated with DANPs, PEG-DANPs, or Tf-PEG-DANPs at 0.001, 0.01, 0.1, 1, 10, and 100 $\mu\text{g}/\text{mL}$ with culture medium only used as a blank control group. After incubation for 48 h, 20 μL of MTT was added per well and further incubated for 4 h. MTT was aspirated off and 180 μL /well of dimethyl sulfoxide was added to dissolve the formazan crystals, and the plate was gently shaken for 10 min. Optical density measurements were performed at 490 nm and the growth inhibition rate of calculated according to the following

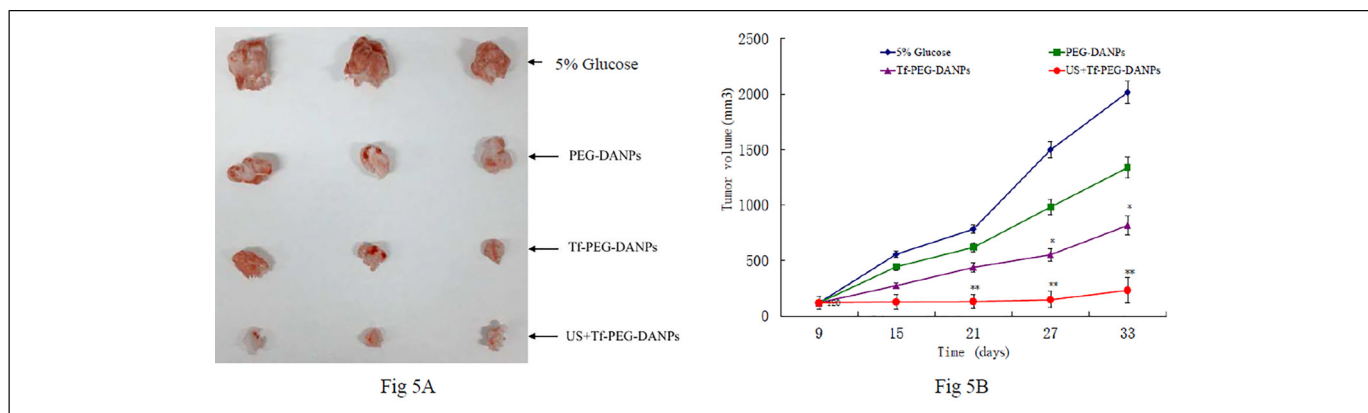


Figure 5. (A and B) Effects of PEG-DANPS, Tf-PEG-DANPS, and US + Tf-PEG-DANPS on 4T1 tumor growth in vivo. 4T1 tumor-bearing mice were treated with control (5% glucose) or the indicated agents via intravenous administration 4 times at 3-day intervals at a dose of 20 mg/kg. Ultrasonic irradiation conditions involved 30 s per time at the intensity of 1 MHz. Changes in the tumor volume in (A) a, b and in (B) c, d treatments. The tumor volume of the US + Tf-PEG-DANPS group was significantly smaller than other groups ($*P < .05$, $**P < .01$). Abbreviations: PEG-DANPS: docetaxel-loaded pegylated-albumin nanoparticles; Tf-PEG-DANPS: transferrin-PEG-DANPS; US + Tf + PEG-DANPS, Tf-PEG-DANPS combined with US.

formula: Cell inhibition (%) = $\frac{[(OD_{\text{sample}} - OD_{\text{blank}}) - (OD_{\text{drug}} - OD_{\text{blank}})]}{(OD_{\text{sample}} - OD_{\text{blank}})} \times 100\%$.¹²

Apoptosis Assays

Apoptotic cells were determined by dual staining with an Annexin V and propidium iodide (PI) kit (4A Biotech) according to the manufacturer's instructions.¹³ After 48 h of incubation in the exponential stage, 4T1 cells growing at ~60% density were treated with 10 $\mu\text{g/mL}$ DANPS, PEG-DANPS, or Tf-PEG-DANPS, respectively. After treatment, cells were washed twice with warm PBS, detached by trypsin without ethylenediaminetetraacetic acid, then through the following steps:

collection, centrifugation, washing with warm PBS, further staining with PI, and Annexin V-fluorescein isothiocyanate (Annexin V-FITC) for 15 min at room temperature in the dark. Apoptosis was then analyzed using a FACScan cytometer (Toshiba). Quadrant analysis was performed and cells that stained positive for both Annexin V-FITC and PI were designated as apoptotic, while unstained cells were designated as viable.

In Vivo Breast Cancer Model

All experimental procedures were performed in conformity with institutional guidelines and protocols for the care and use of laboratory animals. Twenty mice were divided into 4 groups of 5 mice. Isogenic 4T1 cells were suspended in BD Matrigel, and the mice in each group were subcutaneously implanted with 3×10^6 cells to establish the transplantation tumor models previously described.^{14,15} Once the average tumor volumes reached ~120 mm³, mice were treated 4 times at 7-day intervals with either 5% glucose injection (control), PEG-DANPS, Tf-PEG-DANPS, or US + Tf-PEG-DANPS, respectively, for each group. All formulations were injected intravenously via the tail vein at a docetaxel dose of 20 mg/kg.¹³ For the US, we used a low-intensity nonfocusing ultrasonic instrument to irradiate the tumor for 30 s per time at 1 MHz intensity after injection immediately. Bodyweight and tumor volume were measured throughout the experiment and 2 days after the last dose, the mice were sacrificed by cervical dislocation. The tumors, lungs, and other major organs (including heart, liver, spleen, and kidney) were removed, fixed in 10% formalin solution, and subjected to paraffin embedding for H&E staining.^{16,17}

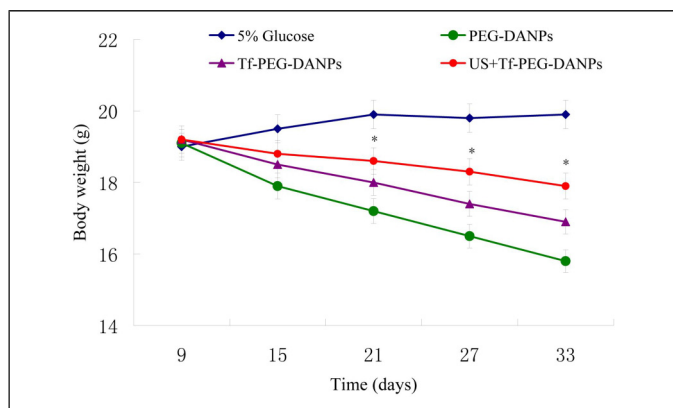


Figure 6. Changes in the bodyweight of 4T1 tumor-bearing mice. The body weights of the mice treated with 5% glucose, PEG-DANPS, Tf-PEG-DANPS, or US + Tf-PEG-DANPS, respectively. The body weights of the US + Tf-PEG-DANPS group were significantly heavier than the other groups ($*P < 0.01$).

Abbreviations: PEG-DANPS, docetaxel-loaded pegylated-albumin nanoparticles; Tf-PEG-DANPS, transferrin-PEG-DANPS; US + Tf + PEG-DANPS, Tf-PEG-DANPS combined with US.

Semiquantitative Analysis of Tissues

H&E sections were used to assess tumor burden in mouse lungs and liver. Semiquantitative scores were determined using the

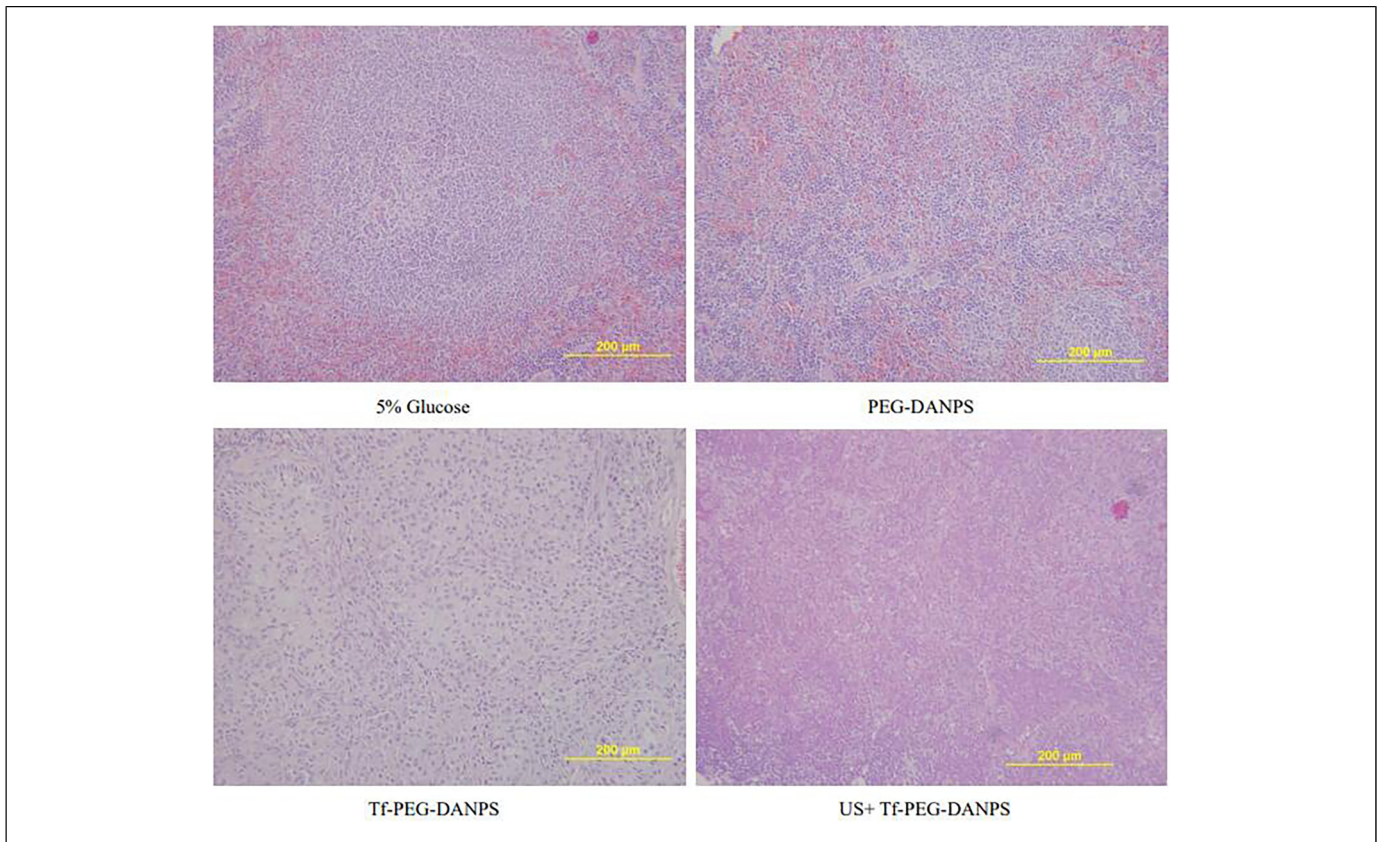


Figure 7. Histological comparisons of 4T1 tumors treated with 5% glucose, PEG-DANPS, Tf-PEG-DANPS, or US + Tf-PEG-DANPS (HE staining at $\times 500$ magnification).

Abbreviations: PEG-DANPS: docetaxel-loaded pegylated-albumin nanoparticles; Tf-PEG-DANPS: transferrin-PEG-DANPS; US + Tf + PEG-DANPS, Tf-PEG-DANPS combined with US; HE, hematoxylin and eosin.

image Analyzer via Image-Pro Plus6.0 analysis system including depth of staining of the cancer cell nucleus, nuclear morphology, atypia, arrangement of cancer cells, formation of tumor emboli in lung alveoli, the formation of cancer nests in liver tissue, the proliferation of fibrous tissue, the bleeding of tissue, the degeneration and necrosis of cancer cells. Each index was rated as 0 (normal) to 3 (abnormal).¹⁸

Statistical Analysis

Results were analyzed by SPSS19.0. Data are presented as mean \pm standard deviation. Significant differences between the 2 groups were evaluated using the Student's *t*-test. Comparisons among multiple groups were performed by 1-way analysis of variance with Bonferroni's post hoc test. A $p < .05$ was considered significant.

Results

Characterization of Nanoparticles

The characterization of Tf-PEG-DANPS has an average particle size of 164.3 ± 2.55 nm (Figure 1), a zeta potential of -19.2 ± 0.16 mV, and a polydispersity index of 0.18 ± 0.04 . The

morphology images of transmission electron microscopy (TEM) indicated that Tf-PEG-DANPS (Figure 2) were spherical with smooth surfaces. According to the results, the particle size of this preparation is suitable, and the distribution is uniform and reasonable. Zeta potential shows that the particle dispersion is stable.

Comparative Effects of Nanomedicine Formulations on Cell Growth in Vitro

We first tested the dose-dependent effects of DANPS, PEG-DANPS, and Tf-PEG-DANPS on the in vitro growth of 4T1 cells. The effects of each formulation in the range of 0.001 to 100 $\mu\text{g}/\text{mL}$ over 48 h were compared. Analysis of the data using the Shapiro–Wilk test confirmed the group data were normally distributed ($s-w = 0.923$, $p = .017$). The results indicated that the Tf-PEG-DANPS formulation was more effective at inhibiting cell proliferation than either DANPS or PEG-DANPS at the lower, more biologically relevant, concentration ranges (0.001 $\mu\text{g}/\text{mL}$, $p = .035$; 0.01 $\mu\text{g}/\text{mL}$, $p = .041$; 0.1 $\mu\text{g}/\text{mL}$, $p = .045$) (Figure 3). However, at the higher concentration ranges (10–100 $\mu\text{g}/\text{mL}$), the effects of Tf-PEG-DANPS were still stronger than DANPS and PEG-DANPS, albeit not significantly

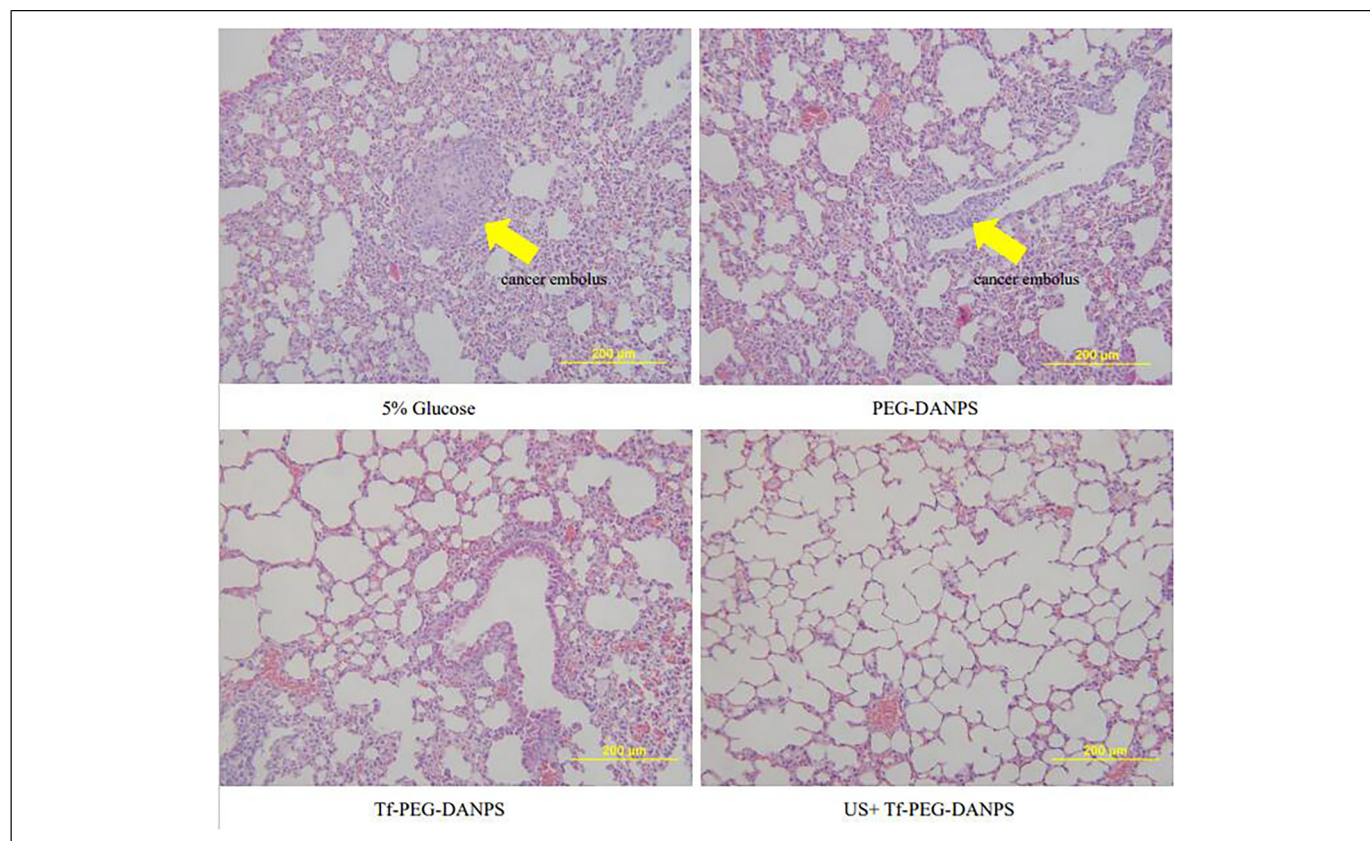


Figure 8. Histological comparisons of lungs from 4T1 tumor-bearing mice treated with 5% glucose, PEG-DANPS, Tf-PEG-DANPS, or US + Tf-PEG-DANPS (HE staining at $\times 500$ magnification).

Abbreviations: PEG-DANPS, docetaxel-loaded pegylated-albumin nanoparticles; Tf-PEG-DANPS: transferrin-PEG-DANPS; US + Tf + PEG-DANPS, Tf-PEG-DANPS combined with US; HE, hematoxylin and eosin.

different ($p = .372$). This suggests that Tf-PEG-DANPS more efficiently targeted breast cancer cells, at least *in vitro*.

Comparative Effects of Nanomedicine Formulations on Cell Apoptosis

We then compared the ability of the nanoparticle formulations to induce apoptosis in 4T1 cells using a flow cytometric assay. As shown in Figure 4, the upper right (Annexin V + PI+) and the lower right quadrant (Annexin V + PI-) populations represent early and late apoptotic cells, respectively. We performed apoptosis assays using Annexin V-FITC and PI staining to compare apoptosis induction. As predicted (see Table 1), Tf-PEG-DANPs (57.89%) increased late apoptosis in A549 cells compared with DANPs and Aisu® (42.95% and 48.23%). Thus, similar to the cell proliferation assays, Tf-PEG-DANPS appeared more efficient at inducing cell apoptosis than either the DANPS and PEG-DANPS formulations.

Antitumor Effects and Toxicity *in Vivo*

The previous experiments established that Tf-PEG-DANPS was more effective than either DANPS or PEG-DANPS in

vitro. Based on these experiments, we then sought to compare the antitumor effects and toxicity of PEG-DANPS versus Tf-PEG-DANPS including an assessment of US treatment combined with the Tf-PEG-DANPS treatment arm. Measurement of tumor size showed both PEG-DANPS and Tf-PEG-DANPS treatments exhibited comparable antitumor effects, but tumor growth in the US + Tf-PEG-DANPS group was more significantly inhibited than either nanomedicine alone (Figure 5). Assessment of body weight as a proxy measure of toxicity indicated decreased body weights compared to control mice for all 3 treatment groups albeit to different degrees. Notably, toxicity in the US + Tf-PEG-DANPS group appeared the least among the treatment groups ($p = .017$) (Figure 6)

In parallel, we undertook a pathological assessment of tissues from the mice at the end of the experiment (Figure 7). Light microscope examination of tumor tissues in the control group showed the adenocarcinoma cell nuclei were hyperchromatic, dark blue, deformed, heterogeneous, lumen or solid. For PEG-DANPS, cancer cell nuclei were pale blue but still showed pathological mitotic shapes. For the Tf-PEG-DANPS treated tumors, the nuclear division of cancer cells was decreased, and there was a little bleeding, local degeneration, and necrosis. In contrast, the nuclei of cancer cells in the US + Tf-PEG-DANPS group were red, and there were no obvious

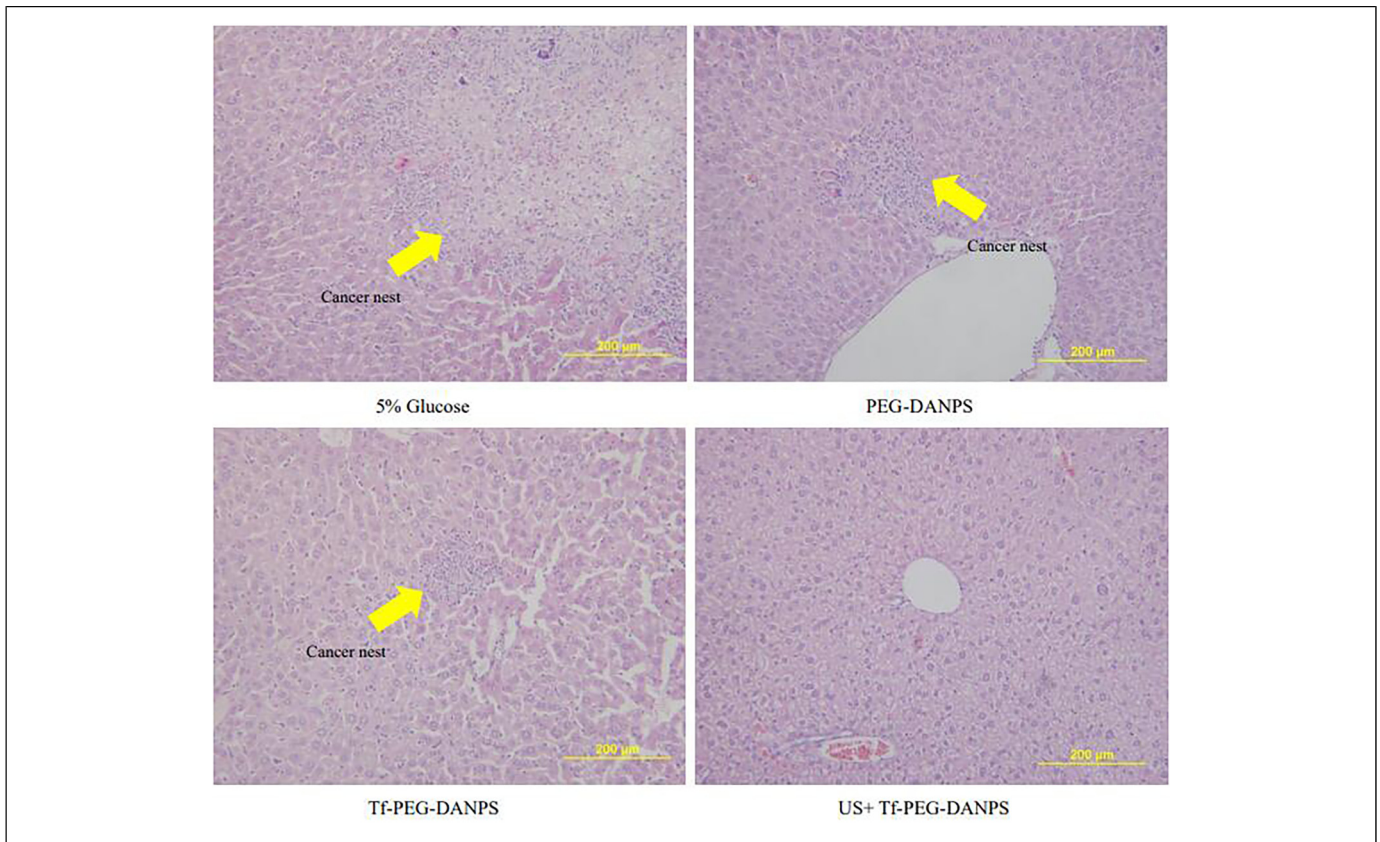


Figure 9. Histological comparisons of livers from 4T1 tumor-bearing mice treated with 5% glucose, PEG-DANPS, Tf-PEG-DANPS, or US + Tf-PEG-DANPS (HE staining at $\times 500$ magnification).

Abbreviations: PEG-DANPS: docetaxel-loaded pegylated-albumin nanoparticles; Tf-PEG-DANPS: transferrin-PEG-DANPS; US + Tf + PEG-DANPS, Tf-PEG-DANPS combined with US; HE, hematoxylin and eosin.

mitotic figures. Moreover, large sheets of cancer cells were denatured and necrotic, together suggesting that the US + Tf-PEG-DANPS combinatorial treatment exhibited the best inhibitory effects on the transplanted tumors.

Investigation of posttreatment lung pathology indicated there were large cancer emboli in the alveoli in the control-treated group (5% glucose injection) group, with cancer cells of obvious atypia (Figure 8). Comparatively smaller emboli were seen in the alveoli of PEG-DANPS treated animals and interestingly, we found no cancer emboli in the Tf-PEG-DANPS group. Similar, there were no tumor cells and only a few normal lung cells with light staining, which showed that US + Tf-PEG-DANPS can inhibit the lung metastasis of breast cancer cells better.

Similar investigations of posttreatment liver pathology indicated a large cancer nest within the liver in the control group, with cancer cell nuclei being hyperchromatic, deformed, and heterogeneous (Figure 9). Many cancer nests were still seen in PEG-DANPS treated livers, albeit reduced in size there were visible pathological mitotic figures. In Tf-PEG-DANPS livers, reduced amounts of pathological mitotic figures were seen, and the size of cancer nests was also reduced. After US + Tf-PEG-DANPS treatment, cancer nuclei were red and without mitotic figures, suggesting that US + Tf-PEG-DANPS

promoted the best inhibitory effect on liver metastasis among the treatments used.

Semiquantitative Analysis of Tumor Mass and Lung and Liver Metastasis

We randomly selected 15 sections each from the primary tumors, lung, and liver tissues of each treatment group, and used these to perform a semiquantitative evaluation using the XXX image analysis system. The results defined by pathological scores indicated that the US + Tf-PEG-DANPS treatment (27.38 ± 5.55) was the most effective compared to the PEG-DANPS (45.15 ± 10.66), Tf-PEG-DANPS (34.65 ± 7.97), and control groups (65.10 ± 9.85) ($p = .019$). This finding suggests that the US + Tf-PEG-DANPS treatment arm produced superior antitumor and antimetastatic effects compared with the other evaluated therapies.

Discussion

Our previous studies showed that PEG-DANPS effectively inhibits the growth and metastasis of nonsmall cell lung cancer. Based on this platform we aimed to improve the efficacy

of PEG-DANPS toward the treatment of breast cancer. Xiang et al.¹⁹ previously reported that the TfR was overexpressed in many tumor types with levels more than 100 times higher than for normal tissues. Prior studies have indicated that Tf-modified paclitaxel-loaded nanoparticles can stably accumulate in lung cancer tissue, improving the targeting and effectiveness of chemotherapy.^{20,21} Exploiting this characteristic, our study incorporated Tf into PEG-DANPS, deriving drug-loaded nanoparticles that would specifically and avidly bind to the surface of tumor cells. Indeed, our results showed clear evidence that Tf-modified PEG-DANPS were more effective than PEG-DANPS in reducing *in vitro* tumor growth. We also showed that Tf-PEG-DANPS had improved antitumor activity and less toxicity compared to PEG-DANPS in a 4T1-based mammary cancer model in mice. This suggests that Tf-PEG-DANPS not only improves tumor targeting but also reduces drug accumulation in normal tissues, and thus potentially represents a great innovation for breast cancer treatment.

In general, PEG-DANPS enters systemic circulation by passive targeting, being swallowed by tissue macrophages of RES in organs such as liver, kidney, and bone marrow, resulting in Docetaxel being concentrated in these organs.^{22,23} However, Docetaxel has significant toxicity, notably causing granulocytopenia, which leads to susceptibility to infection, allergic reactions, and neurotoxicity. These symptoms impair the body's nutritional status leading to body mass decline and then even organ failure.^{24,25} The implications from our study are that Tf-PEG-DANPS acts to directly target tumor cells via the TfR–Tf interaction which in turn, reduces its off-target accumulation, sparing important organs, improving nutritional status, and maintaining body mass. Thus the Tf-PEG-DANPS avoided being sequestered by the RES and transformed into a “stealth” nanoparticle, and the amount of it reaching the tumor cells and absorbed by the tumor cells was significantly increased.²⁶

In addition to comparing the therapeutic effects of PEG-DANPS versus Tf-PEG-DANPS, we also incorporated a third treatment arm involving US+Tf-PEG-DANPS. Other scholars have found the US combined with chemotherapy drugs or nanomedicines can provide beneficial treatment effects the adjuvant treatment of tumors.²⁷ US has been shown to enhance the effectiveness of nanomedicine in treating tumors.²⁸ The principle is mainly based on the cavitation and diffusion effects of the US. Cavitation refers to the large number of vacuum microbubbles produced in the negative pressure region formed by the decompressive action of the fluid in the tumor vessels during US irradiation. When converted to supercharging, these bubbles burst under pressure, creating an impact of more than 1000 air pressure that pushes the drug into the molecular gaps of cancer cells, and play the role in cancer cells.²⁹ Furthermore, cavitation increases the permeability of the cell membrane to K^+ and Ca^{2+} , promoting cell membrane diffusion and permitting drugs to enter more efficiently into cancer cells.³⁰ Secondly, when drug preparations enter cancer cells, the mechanical vibration effect of the US can stimulate the movement of substances within cancer cells, also known as the “massage effect.” Through this effect, drug

preparations oscillate, rub, and circulate in the cytoplasm, which changes the internal structure of cells, thus, drugs can exhibit a more higher anticancer effect.³¹ Finally, there is also a “thermal effect” produced by the US, which can kill tumor cells to a certain extent, which is based on the current clinical application of US knife and other technologies.³² The results of this study showed that the irradiation temperature was not as high as that of the ultrasonic knife, so the effect was negligible. In this study, the thermal effect was mainly reflected in accelerating the local blood and lymphatic circulation of the tumor tissue, accelerating the metabolism, making the drugs more easily penetrate the cells, and improving drug absorption.³³

The US has a high frequency and a short wavelength, so it can travel in a directed straight line for a sufficient distance in a homogeneous medium, and the shorter the wavelength, the more significant this property. Thus, for deep nidi such as cancer emboli in the alveoli and nests in the liver, the US promotes drug penetration deep into tissues by improving blood and lymph circulation and boosting metabolism. In addition, the sonic heat produced can accelerate local blood circulation and metabolism, improve drug absorption by cells.³⁴ In this study, the high-frequency cylinder-shaped probe transmitted US waves in a straight line, which more effectively irradiates the tumor instead of surrounding tissue, so off-target damage would be reduced.

At present, researches on US-assisted treatment of diseases mainly focuses on cavitation of the US, which is not in-depth enough.⁹ However, this paper had analyzed other effects of the US to a certain extent, such as mechanical effect, thermal effect, and dispersion effect, which was 1 of the innovations of this study. In the next step, we plan to make use of the real-time imaging features of the US to selectively irradiate the nourishing blood vessels of the tumor, so that more drugs can be concentrated in the blood supply area of the tumor, to exhibit a better antitumor effect and further improve the efficacy of chemotherapy agents. However, while the results in mice have been relatively satisfactory, further observation and research are needed before the treatment can be used in humans. In summary, the treatment of US combined with Tf-PEG-DANPS may be a new option for the clinical treatment of breast cancer and has a certain promotion prospect.

All animal procedures were approved by the institutional ethics committee (Regulations on Administration and Protection of experimental animals), Yanbian University Hospital under the approval number IACUC-201902022-05. All experiments abided by the Ethical 3R principle.

Acknowledgments

The authors are grateful to EditSprings (<https://www.editsprings.com/>) for the expert linguistic services provided.


Declaration of Conflicting Interests

The authors declared no potential conflicts of interest with respect to the research, authorship, and/or publication of this article.

Funding

The authors disclosed receipt of the following financial support for the research, authorship, and/or publication of this article: This work was funded by the Health and Technology Backbone Project of Jilin Province (2018Q038) and “13th Five-Year Plan” science and technology research project of Jilin Education Department (JKH20191145KJ).

ORCID iD

Guangming Jin  <https://orcid.org/0000-0002-3608-9516>

Supplemental Material

Supplemental material for this article is available online.

References

- DeSantis CE, Ma J, Goding Sauer A, Newman LA, Jemal A. Breast cancer statistics, 2017, racial disparity in mortality by state. *CA-Cancer J Clin.* 2017;67(6):439-448.
- Yang L, Ye L, Zhang YX, Shen WY, Zhou W, Rang WQ. A bibliometric analysis of controllable factors influencing breast cancer in Chinese females. *Pr Prev Med.* 2020;13(4):30-34 (in Chinese).
- Gomez SL, Von Behren J, McKinley M, et al. Breast cancer in Asian Americans in California, 1988-2013: increasing incidence trends and recent data on breast cancer subtypes. *Breast Cancer Res Trans.* 2017;164(1):139-147.
- Robson M, Im SA, Senkus E, et al. Olaparib for metastatic breast cancer in patients with a germline BRCA mutation. *N Eng J Med.* 2017;377(6):523-533.
- Ran R, Liu Y, Gao H, et al. PEGylated hyaluronic acid-modified liposomal delivery system with anti- γ -glutamylcyclotransferase siRNA for drug-resistant MCF-7 breast cancer therapy. *J Pharm Sci-US.* 2015;104(2):476-484.
- Jin GM, Jin MJ, Yin XZ, Jin ZH, Chen LQ, Gao ZG. A comparative study on the effect of docetaxel-albumin nanoparticles and docetaxel-loaded PEG-albumin nanoparticles against non-small cell lung cancer. *Int J Oncol.* 2015;47(5):1945-1953.
- Jin GM, Jin MJ, Jin ZH, Gao ZG, Yin XZ. Docetaxel-loaded PEG-albumin nanoparticles with improved antitumor efficiency against non-small cell lung cancer. *Oncol Rep.* 2016;36(2):871-876.
- Jadia R, Kydd J, Rai P. Remotely phototriggered, transferrin-targeted polymeric nanoparticles for the treatment of breast cancer. *Photochem Photobiol.* 2018;50(4):1004-1015.
- Şenay HŞ, Ak G, Habibe Y, et al. Development of ultrasound-triggered and magnetic-targeted nanobubble system for dual-drug delivery. *J Pharm Sci.* 2019;108(3):1272-1283.
- Percie du Sert N, Hurst V, Ahluwalia A. The ARRIVE guidelines 2.0: updated guidelines for reporting animal research. *Br J Pharmacol.* 2020;177(9):3617-3624.
- Bartley KA, Johnson CH. Human infant pants for postoperative protection during social housing of New Zealand white rabbits (*Oryctolagus cuniculus*). *J Am Assoc Lab Anim.* 2019;58(4):510-516.
- Li JQ, Yang ZZ, Meng TT, Qi XR. The use of cationic liposomes to co-deliver docetaxel and siRNA for targeted therapy of hepatocellular carcinoma. *J Chin Pharm Sci.* 2014;23(10):667-673.
- Li Y, Jin M, Shao S, et al. Small-sized polymeric micelles incorporating docetaxel suppress distant metastases in the clinically-relevant 4T1 mouse breast cancer model. *BMC Cancer.* 2014;14(1):329-344.
- Sakamoto K, Schmidt JW, Wagner KU. Mouse models of breast cancer. *Methods Mol Biol.* 2015;1267(1):47-71.
- Park MK, Lee CH, Lee H. Mouse models of breast cancer in pre-clinical research. *Lab Anim Res.* 2018;34(4):160-165.
- Kim D, Gao ZG, Lee ES, Bae YH. In vivo evaluation of doxorubicin-loaded polymeric micelles targeting folate receptors and early endosomal pH in drug-resistant ovarian cancer. *Mol Pharm.* 2009;6(5):1353-1362.
- Bansal KK, Gupta J, Rosling A, Rosenholm J. Renewable poly (δ -decalactone) based block copolymer micelles as drug delivery vehicle: in vitro and in vivo evaluation. *Saudi Pharm J.* 2018;26(3):358-368.
- Xiang Y, Huang SG, Wan HY, Wu HC. Study on criterion for classifying and quantitating the pathomorphologic changes in the smoker's small airways. *Shanghai Med.* 2005;28(12):1007-1009 (in Chinese).
- Shao ZY, Shao JY, Tan BX, et al. Targeted lung cancer therapy: preparation and optimization of transferrin-decorated nanostructured lipid carriers as novel nanomedicine for co-delivery of anticancer drugs and DNA. *Int J Nanomed.* 2015;10(5):1223-1233.
- Mao JN, Meng XF, Zhao C, Yang YX, Liu GD. Development of transferrin-modified poly (lactic-co-glycolic acid) nanoparticles for glioma therapy. *Anti-Cancer Drug.* 2019;30(6):604-610.
- Zhao S, Zhu X, Cao C, Sun J, Liu J. Transferrin modified ruthenium nanoparticles with good biocompatibility for photothermal tumor therapy. *J Colloid Interface Sci.* 2017;511(9):325-334.
- Handa P, Maliken BD, Nelson JE, et al. Differences in hepatic expression of iron, inflammation and stress-related genes in patients with nonalcoholic steatohepatitis. *Ann Hepatol.* 2017;16(1):77-85.
- Li KS, Liu YH, Zhang SM, et al. Folate receptor-targeted ultrasonic PFOB nanoparticles: synthesis, characterization and application in tumor-targeted imaging. *Int J Mol Med.* 2017;39(6):1505-1515.
- Lin HM, Nikolic I, Yang J, et al. MicroRNAs as potential therapeutics to enhance chemosensitivity in advanced prostate cancer. *Sci Rep.* 2018;8(1):1-12.
- Jin MJ, Jin GM, Huang W, Gao ZG. PEGylation of lumbrokinase improves pharmacokinetic profile and enhances antithrombotic effect in a rat carotid artery thrombosis model. *Mol Med Rep.* 2017;16(4):4909-4914.
- Rizvi SA, Saleh AM. Applications of nanoparticle systems in drug delivery technology. *Saudi Pharm J.* 2018;26(1):64-70.
- Elkhodiry MA, Momah CC, Suwaidi SR, et al. Synergistic nanomedicine: passive, active, and ultrasound-triggered drug delivery in cancer treatment. *J Nanosci Nanotechnol.* 2016;16(1):1-18.

28. Pola A, Montesano L, Tocci M, La Vecchia GM. Influence of ultrasound treatment on cavitation erosion resistance of AISi7 alloy. *Materials*. 2017;10(3):256-266.
29. Fang Y, Georgy S, Chen Y, Zhong P. Probing the bioeffects of cavitation at the single-cell level. *J Acoust Soc Am*. 2013;134(5):3992-4002.
30. Ding W, Wu CS. Effect of ultrasonic vibration exerted at the tool on friction stir welding process and joint quality. *J Manuf Process*. 2019;42(6):192-201.
31. Zhao G, Wang Z, Hu S, et al. Effect of ultrasonic vibration of molten pool on microstructure and mechanical properties of Ti-6Al-4V joints prepared via CMT+P welding. *J Manuf Process*. 2020;52(10):193-202.
32. Wang H, Yuan Y, Chen Y. Characterization and mechanism of accelerated curing of adhesives by in situ ultrasonic vibration for bonded joints. *J Polym Eng*. 2019;40(1):1-12.
33. Lin CY, Chen PY, Shau YW, Wang CL. An artifact in supersonic shear wave elastography. *Ultrasound Med Biol*. 2017;43(2):517-530.
34. Zhang SY, Cui ZW, Li C, et al. Enhanced cavitation and heating of flowing polymer-and lipid-shelled microbubbles and phase-shift nanodroplets during focused ultrasound exposures. *AIP Conf Proc*. 2017;3(1):1-5.